Theoretical Study of Ammonia and Methane Activation by First-Row Transition Metal Cations M + (M = Ti, V, Cr)

ARTICLE *in* JOURNAL OF THE AMERICAN CHEMICAL SOCIETY · FEBRUARY 2002

Impact Factor: 12.11 · DOI: 10.1021/ja0112487

2 AUTHORS:

Emilia Sicilia
Università della Calabria
150 PUBLICATIONS **1,919** CITATIONS
SEE PROFILE

Nino Russo
Università della Calabria
509 PUBLICATIONS **7,856** CITATIONS
SEE PROFILE

J|A|C|S
ARTICLES
Published on Web 01/25/2002

Theoretical Study of Ammonia and Methane Activation by First-Row Transition Metal Cations M^+ (M = Ti, V, Cr)

Emilia Sicilia* and Nino Russo*

Contribution from the Dipartimento di Chimica and Centro di Calcolo ad Alte Prestazioni per Elaborazioni Parallele e Distribuite-Centro d'Eccellenza MIUR, Università della Calabria, I-87030 Arcavacata di Rende, Italy

Received May 22, 2001. Revised Manuscript Received August 27, 2001

Abstract: The potential energy surfaces for the reaction of first-row transition metal cations $Ti^+(^4F,^2F)$, $V^+(^5D,^3F)$, and $Cr^+(^6S,^4D)$ with NH_3 and CH_4 have been built up by using density functional theory. In all cases, the high-spin ion−dipole complex, which is the most stable species on the respective potential energy hypersurfaces, is initially formed. In the second step, a hydrogen shift process leads to the formation of the insertion products, which are more stable in a low-spin state. From these intermediates three dissociation channels have been considered. All the results have been compared with existing experimental and theoretical data and our earlier work on the reactivity of Sc^+, to clarify similarities and differences in the behavior of the transition metal ions considered.

1. Introduction

In the framework of organometallic chemistry many theoretical and experimental approaches have been used to enlighten the details of the reactions of atomic transition metals with small molecules containing prototype bonds (e.g., C−H, C−C, N−H, and O−H). The growing interest in these kinds of reactions has been prompted by their importance in catalytic processes.[1−26] Among the approaches used gas-phase experiments, mass spectrometric in particular, give the opportunity to obtain valuable information on elementary reactions and mechanisms in a controlled environment without disturbing factors. However, from an experimental point of view a complete elucidation of the detailed mechanisms is, often, not possible and a close interaction between theory and experiment is highly desirable. This interaction has already begun to yield results in the case of the study of first-row transition metal cations with water interactions[27−30] and of scandium ion with water, ammonia, and methane.[31]

Experimentally it has been shown that, as well as for the scandium ion,[13,19] the H_2 elimination process is the most thermodynamically favored in the reaction of early (Ti^+ and V^+) and middle (Cr^+) first-row transition metal cations with ammonia and methane, while at higher energies other reaction products become accessible.[5,7−9,15,18,19] It has been suggested that the studied reactions proceed via oxidative addition, i.e., insertion of M^+ (M = Sc, Ti, V, Cr) into the H−X (X = N, C) bond, to form an insertion intermediate that may lie either lower or higher in energy than the reactants.

Comparison between the proposed paths shows that, while the mechanisms of reaction with NH_3 and CH_4 are similar, the energetics are significantly different. The observed similarities have been explained as a result of the fact that ammonia and methane are isoelectronic in the sense that the central heavy atom has the same number of valence electrons with the same sp^3 hybridization.[32] The differences in energetics have been

* Address correspondence to either author.

(1) Freas, R. B.; Ridge, D. P. *J. Am. Chem. Soc*. **1980**, *102*, 7129.
(2) Aristov, A.; Armentrout, P. B *J. Am. Chem. Soc*. **1984**, *106*, 4065.
(3) Tolbert, M. A.; Beauchamp, J. L. B. *J. Am. Chem. Soc*. **1984**, *106*, 8117.
(4) Reents, W. L.; Strobel, F.; Freas, R. B.; Wronka, J.; Ridge, D. P. *J. Phys. Chem*. **1985**, *89*, 5666.
(5) Aristov, N.; Armentrout, P. B. *J. Phys. Chem*. **1986**, *108*, 1806.
(6) Kang, N.; Beauchamp, J. L. *J. Am. Chem. Soc*. **1986**, *108*, 7502.
(7) Aristov, N.; Armentrout, P. B. *J. Phys. Chem*. **1987**, *91*, 6178.
(8) Sunderlin, L. S.; Armentrout, P. B. *J. Phys. Chem*. **1988**, *92*, 1209.
(9) Georgiadis, R.; Armentrout, P. B. *J. Phys. Chem*. **1988**, *92*, 7067.
(10) Tonkyn, R.; Ronan, M.; Weisshaar, J. C. *J. Phys. Chem*. **1988**, *92*, 92.
(11) Buckner, S. W.; Gord, J. R.; Freiser, B. S. *J. Am. Chem. Soc*. **1988**, *110*, 6606.
(12) Irikura, K. K.; Beauchamp, J. L. *J. Am. Chem. Soc*. **1989**, *111*, 75.
(13) Sunderlin, L. S.; Armentrout P. B. *J. Am. Chem. Soc*. **1989**, *111*, 3845.
(14) Magnera, T. F.; David, D. E., Michl, J. *J. Am. Chem. Soc*. **1989**, *111*, 4100.
(15) Armentrout, P. B.; Beauchamp, J. L. *Acc. Chem. Res*. **1989**, *22*, 315.
(16) Russel, D. H, Ed. *Gas-Phase Inorganic Chemistry*; Plenum: New York, 1989; p 412.
(17) Armentrout, P. B. *Annu. Rev. Phys. Chem*. **1990**, *41*, 313.
(18) Clemmer, D. E.; Sunderlin, L. S.; Armentrout, P. B. *J. Phys. Chem*. **1990**, *94*, 208.
(19) Clemmer, D. E.; Sunderlin, L. S.; Armentrout, P. B. *J. Phys. Chem*. **1990**, *94*, 3008.
(20) Armentrout, P. B. *Science* **1991**, *41*, 175.
(21) Fisher, E. R.; Armentrout, P. B. *J. Am. Chem. Soc*. **1992**, *114*, 2049.
(22) Guo, B. C.; Kerns, K. P.; Castleman, A. W. *J. Phys. Chem*. **1992**, *96*, 4879.
(23) Clemmer, D. E.; Aristov, N.; Armentrout, P. B. *J. Phys. Chem*. **1993**, *97*, 544.
(24) Chen, Y.; Clemmer, D. E.; Armentrout, P. B. *J. Phys. Chem*. **1994**, *98*, 11490.
(25) Chen, Y.; Armentrout, P. B. *J. Phys. Chem*. **1995**, *99*, 10775.
(26) Haynes, C. L.; Chen, Y.; Armentrout, P. B. *J. Phys. Chem*. **1995**, *99*, 9110.
(27) Irigoras, A.; Fowler, J. E.; Ugalde, J. M. *J. Phys. Chem*. **1998**, *102*, 293.
(28) Irigoras, A.; Fowler, J. E.; Ugalde, J. M. *J. Am. Chem. Soc*. **1999**, *121*, 574.
(29) Irigoras, A.; Fowler, J. E.; Ugalde, J. M. *J. Am. Chem. Soc*. **1999**, *121*, 8549.
(30) Irigoras, A.; Elizalde, O.; Silanes, I.; Fowler, J. E.; Ugalde, J. M. *J. Am. Chem. Soc*. **2000**, *122*, 114.
(31) Russo, N.; Sicilia, E. *J. Am. Chem. Soc*. **2001**, *123*, 2588.
(32) Bent, H. A. *J. Chem. Educ.* **1966**, *43*, 170.

attributed[18,19] to the different numbers of lone pairs: that is, one on the nitrogen atom of ammonia and none on the carbon atom of methane. On the other hand, differences in the behavior of the considered cations are induced by the different atomic orbital occupancies, which dictate the accessibility of metal orbitals to electron donation from the ligand.

Another topic of interest in these reactions is the influence of the electronic state of the metal cation upon the reactivity and reaction path. The hypothesis of a crossing between high- and low-spin surfaces, probably occurring in the region of the ion−molecule complex, $M^{+-}XH_n$ (X = N, C), has been proposed[7−9,17,18] to explain the nature of the final products with respect to the reactants and the efficiency of the reaction.

We will summarize briefly the previous theoretical and experimental work in the literature on the dehydrogenation reaction of methane and ammonia by Ti^+, V^+, and Cr^+. Experimentally, the study of the reaction of the chromium ion (generated by electron impact) with methane, performed by Reents et al.[4] using ion cyclotron resonance spectrometry, is pertinent to this work. Guided ion beam mass spectrometry was used by Armentrout et al. to study the activation of methane by titanium,[8] vanadium,[7] and chromium[9] cations. The gas-phase reactions of first-row transition metal ions, from Sc^+ to Zn^+, with small alkanes, including methane, were studied in the multicollisional environment of a fast flow reactor.[10] The interaction of V^+ and Cr^+ with ammonia was studied by Buckner et al.[11] using a Fourier transform ion cyclotron. The reaction of Ti^+ and V^+ with NH_3 was also studied by Armentrout et al.[18,19] by means of an ion-beam apparatus. The chemistry and kinetics, at room temperature, of the reaction of Ti^+ with NH_3 were studied by Guo et al.[22] applying the selected ion drift tube technique coupled to a laser vaporization source. Finally, bond dissociation energies (BDEs) of M^+-NH_3 complexes of first-row transition metals have been determined by examining their collision-induced dissociation reactions.[33]

On the theoretical side, an MP4(SDTQ)/6-31G**//MP2/6-31G** study of the insertion reaction into CH_4 and NH_3 of the titanium ion in its ^2F excited state was carried out by Song and Chaojie.[34] The CASSCF method combined with gradient techniques has been used to study the stability of the low-spin hydridomethyl complexes, $H-M^+-CH_3$, of the first-row transition metal cations.[35] Geometries, electronic structures, and binding energies of these species, which are assumed as stable intermediates in the insertion reactions into the C−H bond, have been reported together with those of the transition states leading to them. The properties of the adducts formed upon interaction of ammonia with the ions of interest have been calculated by using a modified extended Hückel molecular orbital model,[36] and their binding energies were also determined using the modified coupled-pair functional approach.[37] The nonsystematic approach of these works does not help to clarify the interaction mechanism and to obtain a homogeneous picture of the potential energy profiles. Therefore, a systematic theoretical study of the above reactions at the same level of theory would be very useful.

In this paper we continue our density functional (DF) study, begun with the scandium ion in both its singlet and triplet states,[31] of the potential energy hypersurfaces for the reactions

$$M^+ + XH_n \rightarrow MXH_{n-2}^+ + H_2 \ (M = Ti, V, Cr) \quad (1)$$

$$\rightarrow MH^+ + XH_{n-1} \ (X = N, C) \quad (2)$$

$$\rightarrow MXH_{n-1}^+ + H \quad (3)$$

The full reaction mechanism, geometries, and energetics for both the high- and low-spin states of the ions, considering the possible transition states, have been considered.

Due to the presence in the literature of the extensive studies of Ugalde et al. on the mechanism of the reactions between first-row transition metal ions and water,[27−30] the influence of different small ligands on the reactivity of the same metal center can be investigated.

2. Method

The computational method used for geometry optimization and frequency calculations was density functional (DF) theory in its B3LYP[38,39] formulation with the DZVP (for the transition metals) and TZVP (for the other atoms) sets given by Goudbot et al.[40] The TZVP basis sets, previously used by Ugalde et al.[27−30] for the metals, have also been employed to check the influence of the basis set size on the reliability of the energy difference between the ground state and the excited state of the metal ions. The choice of the B3LYP DF method is motivated by its usefulness as a practical tool in describing even complex situation such as those present in open-shell transition metal compounds.[41−46] Moreover, previous work on this subject[27−30,42,47,48] underlines the reliability of DF methods, in their B3LYP formulation, to describe potential energy surfaces (PESs) for reactions involving Ti, V, and Cr ions. It is noteworthy that for some reactions involving radical hydrogen abstraction the B3LYP functional tends to underestimate barrier heights and should be used with caution.[49,50] The reactions taken into account in the present work do not involve transition states for atomic hydrogen abstraction, so these failures would be less probable. Moreover, a comparison between DF[31,51] and MR-SDCI-CASSCF[52,53] PESs for reactions of Sc^+ and Co^+ with methane show similar barrier heights.

For each optimized stationary point vibrational analysis was performed to determine its character (minimum or saddle point) and to evaluate the zero-point vibrational energy (ZPE) corrections, which are included in all relative energies.

(33) Walter, D.; Armentrout, P. B. *J. Am. Chem. Soc*. **1998**, *120*, 3176.
(34) Chaojie, W.; Song, Y. *Int. J. Quantum Chem.* **1999**, *75*, 47.
(35) Hendrickx, M.; Ceulemans, M.; Gong, K.; Vanquickenborne, L. *J. Phys. Chem*. **1997**, *101*, 2465.
(36) Tsipis, A. C. *J. Chem. Soc., Faraday Trans.* **1998**, *94*, 11.
(37) Langhoff, S. R.; Bauschlicher, C. W.; Partridge, H.; Sodupe, M. *J. Phys. Chem*. **1991**, *95*, 10677.
(38) Becke, A. D. *J. Chem. Phys.* **1993**, *98*, 5648.
(39) Lee, C.; Yang, W.; Parr, R. G. *Phys. Rev. B* **1988**, *37*, 785.
(40) Goudbout, N.; Salahub, D. R.; Andzelm, J.; Wimmer, E. *Can. J. Chem*. **1992**, *70*, 560.
(41) Davidson, E. R. *Chem. Rev*. **2000**, *100*, 351.
(42) Aschi, M.; Bronstrup, M.; Diefenbach, M.; Harvey, J. N.; Schroder, D.; Schwarz, H. *Angew. Chem., Int. Ed.* **1998**, *37*, 829.
(43) Halthausen, M. C.; Fiedler, A.; Schwarz, H.; Koch, W. *J. Phys. Chem*. **1996**, *100*, 6236.
(44) Bauschlicher, C. W., Jr.; Ricca, A.; Partridge, H.; Langghoff, S. R. In *Recent Advances in Density Functional Theory*; Chong, D. P., Ed.; World Scientific Publishing Co.: Singapore, 1997; Part II and references therein.
(45) Sodupe, M.; Branchadell, V.; Rosi, M.; Bauschlicher, C. W., Jr. *J. Phys. Chem*. **1997**, *101*, 7854.
(46) Pavlov, M.; Siegbahn, P. E. M.; Sandström, M. *J. Phys. Chem*. *A* **1998**, *102*, 219.
(47) Irigoras, A.; Ugalde, J. M.; Lopez, X.; Sarasola, C. *Can. J. Chem*. **1996**, *74*, 1824.
(48) Yi, S. S.; Blomberg, M. R. A.; Siegbahn, P. E. M.; Weisshaar, M. *J. Phys. Chem*. **1998**, *102*, 395.
(49) Durant, J. L. *Chem. Phys. Lett*. **1996**, *256*, 595.
(50) Jursic, B. S. *Chem. Phys. Lett*. **1997**, *264*, 113.
(51) Abashkin, Y. G.; Burt, S. K.; Russo, N. *J. Phys. Chem*. **1997**, *101*, 8085.
(52) Musaev, D. G.; Morokuma, K. *J. Phys. Chem*. **1996**, *100*, 11600.
(53) Musaev, D. G.; Morokuma, K.; Koga, N.; Nquyen, K. A.; Gordon, M. S.; Cundari, T. R. *J. Phys. Chem*. **1993**, *97*, 11435.

Table 1. Relative Energies, in kcal/mol, of the M^+ Excited State with Respect to Ground State

cation	configurations (state)	B3LYP/DZVP	B3LYP/TZVP	expt[a]
Ti^+	sd^2 (^{4}F)−sd^2 (^{2}F)	12.92	12.57	13.67
V^+	d^4 (^{5}D)−sd^3 (^{3}F)	22.52	21.28	25.37
Cr^+	d^5 (^{6}D)−sd^4 (^{4}D)	53.13	52.18	56.73

[a] Reference 48.

A full natural bond orbital (NBO) analysis[54,55] was performed at some of the stationary points along the low-energy paths to give further insight into their bonding properties.

All the calculations reported here have been carried out with the GAUSSIAN94/DFT[56] code.

3. Results and Discussion

Experimentally,[57] the ground state of Ti^+ is ^{4}F (sd^2) with the secondary excited state of interest ^{2}F (sd^2) lying 13.03 kcal/mol above. For the vanadium ion the electronic ground-state configuration is ^{5}D (d^4), the excited state ^{3}F (sd^3) being 24.77 kcal/mol higher in energy. The excitation energy between the ground ^{6}D (d^5) and the secondary ^{4}D (sd^4) excited state of Cr^+ is 56.73 kcal/mol. In Table 1 the results obtained for the excitation energies of the above-mentioned cations are reported. Even though excitation energies of transition metal atoms and ions are notoriously difficult to compute accurately using DF approaches,[58,59] the agreement between our data, at both levels of theory employed, and the experimental data is satisfactory. All the values are lower than those given by Moore,[57] the high−low-spin splitting of Cr^+ being more underestimated. However, the differences are small enough for a reliable assignment of the ionic states and a correct understanding of the PESs, as previously pointed out by Irigoras et al.[27,29]

Moreover, these results confirm that DZVP basis set can be confidently used, the agreement with experiment being of the same order as that achieved by using the more extended TZVP basis set.

According to experimental observations[5,7−9,18,19,22] the reaction of metal ions, M^+ (M = Ti, V, Cr), with ammonia and methane (XH_n (X = C, N)) are expected to form, in the first step, a stable ion−dipole complex. The reasonable mechanisms for the next H−X bond breaking step are M^+ insertion into an H−X bond to form an $H-M^+-XH_{n-1}$ intermediate, or direct abstraction of one H atom from XH_n. The first process is thermodynamically more favorable since the broken H−X bond energy is replaced by the energy of the $H-M^+$ and M^+-XH_{n-1} bonds formed. The reaction, then, can proceed toward the formation of dehydrogenation products, through a concerted four-center elimination of H_2, or formation of MH^+ and MXH_{n-1} species, as a result of simple cleavage of M−X and M−H bonds in the insertion intermediate.

Table 2. Relative Energies of M^+-NH_3 (ΔE), HM^+-NH_2 (ΔE_1), and $MNH^+ + H_2$ (ΔE_2) Products with Respect to the Ground State of Reactants[a]

system	method	ΔE	ΔE_1	ΔE_2
$Ti^+(^4F) + NH_3$	B3LYP/DZVP[b]	−52.86	−30.58	−9.75
	MCPF[c]	−47.0		
	MP4//MP2[d]	−102.8	−101.2	
	expt	−46.58 ± 1.61[e]	−32.28[f]	−15.0 ± 2.8[f]
$V^+(^5D) + NH_3$	B3LYP/DZVP[b]	−47.83	−13.84	0.41
	MCPF[c]	−46.5		
	expt	−44.50 ± 1.84[e]	−13.84[g]	−2.77[g]
$Cr^+(^6D) + NH_3$	B3LYP/DZVP[b]	−45.03	8.48	28.52
	MCPF[c]	−41.8		
	expt	−43.58 ± 2.31[e]		

[a] Ground states of the products are Ti^+-NH_3 (^{4}A), $H-Ti^+-NH_2$ (^{2}A), $TiNH^+$ (^{3}A), V^+-NH_3 (^{5}A), $H-V^+-NH_2$ (^{3}A), VNH^+ (^{3}A), Cr^+-NH_3 (^{6}A), $H-Cr^+-NH_2$ (^{4}A), and $CrNH^+$ (^{4}A). [b] The basis sets refer to the metal atom. [c] Reference 35. [d] Reference 32. These values of ΔE are calculated with respect to the doublet excited state of the reactants. [e] Reference 31. [f] Reference 18. [g] Reference 17.

An alternative proposed[5,7−9,18,19] mechanism involves, for the H_2 elimination (reaction 1), the formation of the insertion intermediate followed by α-H migration to M^+ to form $(H)_2-M^+-XH_{n-2}$ and reductive elimination of H_2. On the basis of thermochemical arguments, the formation of this intermediate, in which hydrogen atoms are covalently bonded to the metal, can be ruled out, although the formation of the ion−molecule $(H_2)M^+-XH_{n-2}$ complex is not excluded in the exit channel of the molecular hydrogen.

Because of the very strong electronic state dependence of the experimental observations, for each metal cation it is necessary to properly describe the potential energy surfaces for both the ground high-spin state and for the excited one with a configuration compatible with the spin state of the key intermediate $H-M^+-XH_{n-1}$.

3.1. M^+ Insertion into N−H Bond. On the basis of experimental observations[11,18,19,22] and of our results obtained in the case of reaction of the Sc^+ ion,[31] the only reaction pathway we consider for the dehydrogenation of ammonia is that occurring via oxidative addition of the N−H bond, for both high- and low-spin energy surfaces. Geometric parameters of stationary points are reported in Figure 1 for titanium, Figure 2 for vanadium, and Figure 3 for chromium, while their corresponding potential energy profiles are depicted in Figure 4.

Three main ionic products have been considered in the reaction of Ti^+ (^{4}F) and (^{2}F), V^+ (^{5}D) and (^{3}F), and Cr^+ (^{6}D) and (^{4}D):

$$M^+ + NH_3 \rightarrow MNH^+ + H_2 \quad (4)$$

$$M^+ + NH_3 \rightarrow MNH_2^+ + H \quad (5)$$

$$M^+ + NH_3 \rightarrow MH^+ + NH_2 \quad (6)$$

The relative energy data are compared with previous theoretical[34,37] and experimental[18,19,33] results in Tables 2 and 3.

The first step of the reaction is, as previously pointed out, the exothermic formation of the ion−molecule complex (**I**), along both high- and low-spin PESs, with C_s symmetry, which differs only slightly from C_{3v} because of the Jahn−Teller effect.

(54) Carpenter, J. E.; Weinhold, F. *J. Mol. Struct. (THEOCHEM)* **1988**, *169*, 41.
(55) Carpenter, J. E.; Weinhold, F. J. *The Structure of Small Molecules and Ions*; Plenum: New York, 1988.
(56) Frisch, M. J.; Trucks, G. W.; Schlegel, H. B.; Gill, P. M. W.; Johnson, B. G.; Robb, M. A.; Cheeseman, J. R.; Keith, T. A.; Petersson, G. A.; Montgomery, J. A.; Raghavachari, K.; Al-Laham, M. A.; Zakrzewski, V. G.; Ortiz, J. V.; Foresman, J. B.; Croslowski, J.; Stefanov, B. B.; Nanayakkara, A.; Challacombe, M.; Peng, C. Y.; Ayala, P. Y.; Chen, W.; Wong, M. W.; Andres, J. L:, Peplogle, E. S.; Gomperts, R.; Martin, R. L.; Fox, D. J.; Binkley, J. S.; Defrees, D. J.; Baker, J.; Stewart, J. P.; Head-Gordon, M.; Gonzales, C.; Pople, J. A. *Gaussian 94*, revision A.1; Gaussian, Inc.: Pittsburgh, PA, 1995.
(57) Moore, C. E. *Atomic Energy Levels*; NSRD-NBS, USA; US Government Printing Office: Washngton, DC, 1991; Vol. 1.
(58) Parr, R. G.; Yang, W. *Density-Functional Theory of Atoms and Molecules*; Oxford University Press: Oxford, 1989.
(59) Kryachko, E. S.; Ludenã, E. V. In *Energy Density Functional Theory of Many-Electron Systems*; Kluwer: Dordrecht, 1990.

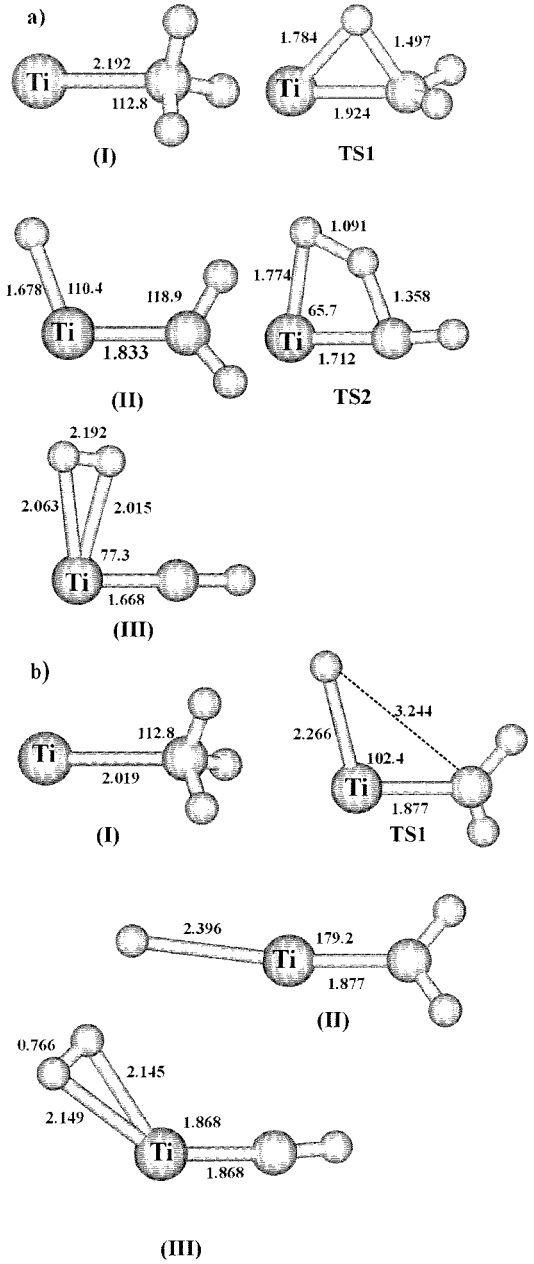

Figure 1. Geometric parameters of minima and transition states on the B3LYP/DZVP doublet (a) and quadruplet (b) potential energy surfaces for the reaction of Ti^+ with NH_3. Bond lengths are in angstroms and angles in degrees.

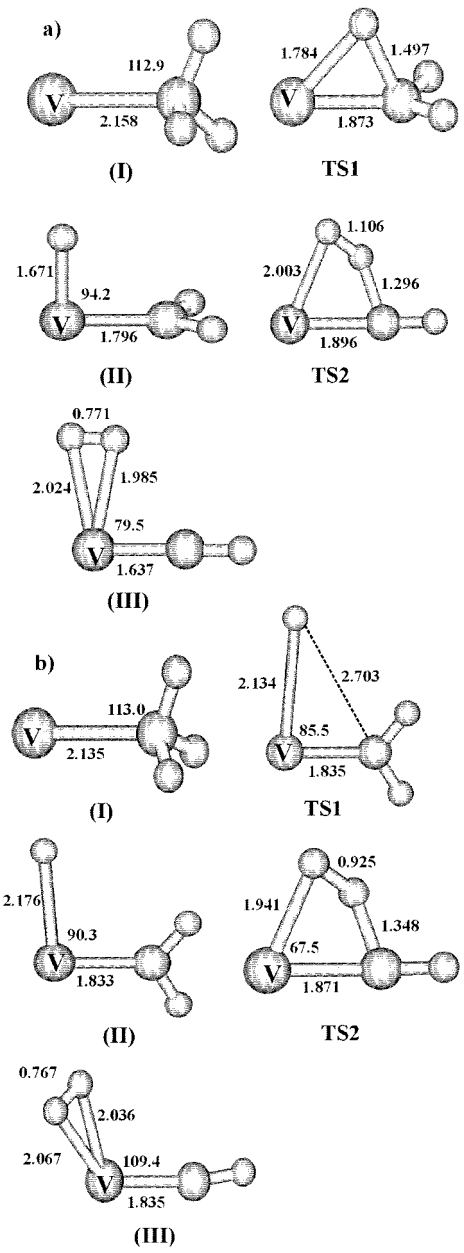

Figure 2. Geometric parameters of minima and transition states on the B3LYP/DZVP triplet (a) and quintuplet (b) potential energy surfaces for the reaction of V^+ with NH_3. Bond lengths are in angstroms and angles in degrees.

As seen in Table 2, the stabilization energy, with respect to the reactants, of the ground-state complex (**I**) is found to be −52.86, −47.83, and −45.03 kcal/mol for titanium, vanadium, and chromium, respectively. The agreement with experimental and CI results is good in the case of V and Cr, but less satisfactory for Ti, for which the difference between experiment and theory is 6.28 kcal/mol. This is a manifestation of the well-known shortcomings of the B3LYP approach: i.e., the tendency to overestimate binding energy[60] and the occurrence of large errors in the calculations for atoms.[61,62]

The next step of the reaction is the insertion of M^+ into the N−H bond of ammonia through the formation of a transition state TS1, which corresponds to the shift of a hydrogen atom from nitrogen to the metal. We succeeded in locating the structures, which are three-center complexes, of the transition states related to this process for all the cations in both their high- and low-spin states. As we can see in Figures 1b, 2b, and 3b, while the topologies of the high-spin transition states are very similar to each other, the large distances between nitrogen and the shifting hydrogen differ significantly in going from Ti^+ to Cr^+ (3.244, 2.703, and 2.936 Å, respectively).

From Figure 4 it is evident that, for all the considered reactions, this region of the potential energy surface is crucial because of a surmised crossing between the two PESs with different electronic spin multiplicity.

(60) Koch, W.; Holthausen, M. C. *A Chemists Guide to Density Functional Theory*; Wiley-VCH: Weinheim, 2000.
(61) Halthausen, M. C.; Mohr, M.; Koch, W. *Chem. Phys. Lett.* **1995**, *240*, 245.
(62) Halthausen, M. C.; Heinemann, C.; Cornehl, H. H.; Koch, W.; Schwarz, H. *J. Chem. Phys.* **1995**, *102*, 4931.

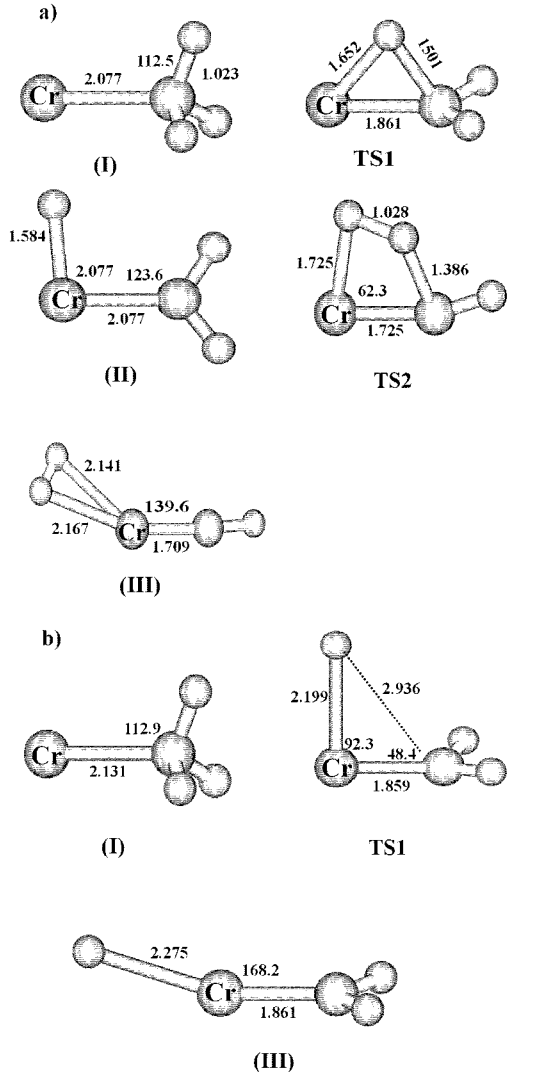

Figure 3. Geometric parameters of minima and transition states on the B3LYP/DZVP quadruplet (a) and sextet (b) potential energy surfaces for the reaction of Cr^+ with NH_3. Bond lengths are in angstroms and angles in degrees.

Table 3. Relative Energies of $M^+-NH_2 + H$ (ΔE) and $MH^+ + NH_2$ (ΔE_1) Products with Respect to the Ground State of the Reactants[a]

system	method	ΔE	ΔE_1
$Ti^+(^4F) + NH_3$	B3LYP/DZVP[b]	12.67	55.90
	expt	23.1 ± 3.0[c]	55.3 ± 2.8
$V^+(^5D) + NH_3$	B3LYP/DZVP[b]	24.70	59.87
	expt	34.82 ± 2.3[d]	60.18 ± 2.1
$Cr^+(^6D) + NH_3$	B3LYP/DZVP[b]	44.39	69.46

[a] Ground states of the products are Ti^+-NH_2 (^3B) + H (^2S), TiH^+ ($^3\Delta$) + NH_2 (^2A), V^+-NH_2 (^4B) + H (^2S), VH^+ ($^4\Delta$) + NH_2 (^2A), Cr^+-NH_2 (^5B) + H (^2S), and CrH^+ ($^5\Delta$) + NH_2 (^2A). [b] The basis sets refer to the metal atom. [c] Reference 18. [d] Reference 17.

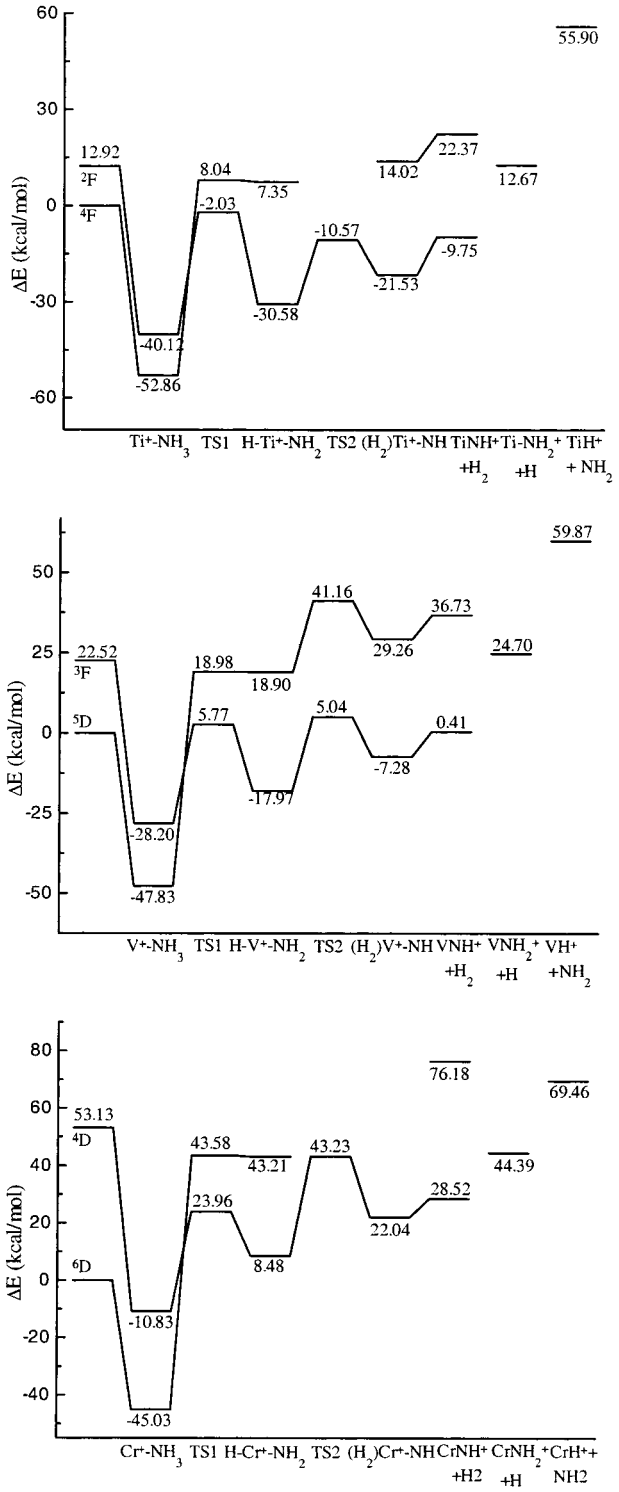

Figure 4. B3LYP/DZVP high- and low-spin potential energy surfaces for the reaction of Ti^+, V^+, and Cr^+ with CH_4. Energies are in kcal/mol and relative to the ground-state reactants.

The insertion intermediate (**II**), although not observed experimentally, is a key structure for understanding the entire reaction mechanism. Indeed for $H-M^+-NH_2$, containing covalent H−M and M−N bonds, two of the valence electrons of the metal are involved in bonding, leading to a low-spin ground state for this species. In the case of Ti and V cations it is possible to compare our data concerning the stability of the intermediates with the estimated values obtained by using bond additivity arguments. The agreement with our results is very satisfactory in both cases, and we can propose for chromium intermediate an endothermicity of 8.48 kcal/mol with respect to the ground-state reactants (see Figure 4).

From the insertion intermediate (**II**) the reaction proceeds to yield the molecular hydrogen complex $(H_2)M-NH^+$ (**III**) after passing through the TS2 four-center transition state. Looking at the barrier heights, it is worth noting that to obtain vanadium

and chromium intermediates, particularly for the latter one, it is necessary to surmount an activation barrier in excess of the endothermicity of the ground state reactants limit. This result for vanadium ion does not agree with experimental observations that suggest, on the basis of a bond additivity estimate, that the formation of this species does not require energy in excess of the reactants.[18]

Finally, the dehydrogenation products are formed directly from (**III**) without an energy barrier. The potential energy behavior from the $M(NH_3)^+$ complex to product formation is very different (see Figure 4) between high- and low-spin states. Indeed, along the high-spin-state reaction path, the formation of all the species is endothermic with respect to the reactants. In particular, because of the very small difference in energy between the insertion product and the transition state leading to it, the existence of this species cannot be established. Thus, this process is not likely to take place under normal conditions. Location of transition state TS2 was successful only along the high-spin path for vanadium ion, and in the case of chromium not even the molecular hydrogen complex was found. Since, as seen in Figure 4, the PESs of reaction for high- and low-spin states cross in the vicinity of the collision complex (**II**), the obvious conclusion, in agreement with experimental hypotheses,[17,18] is that the reaction is a spin-forbidden process that starts with the ion in its high-spin state and finishes with MNH^+ in the low one. The need to undergo an intersystem crossing can be invoked to explain the inefficiency of the process dominated by high-spin ions, as previously noted by experimentalists.[18,19]

For the endothermic production of MNH_2^+ and MH^+ species the ground state of the products is compatible with both high- and low-spin state of the reactants. Thus, formation of MNH_2^+ and MH^+ products would not be as sensitive to the reactant state as the dehydrogenation process. However, due to the low stability of the intermediate (**II**) in its high-spin state, it may be argued that the reaction proceeds, predominantly, through intermediate (**II**) along the low-spin potential energy surface, as is confirmed by the strong state dependence experimentally observed.[18,19]

Concerning the values of the relative energies reported in Tables 2 and 3, we observe that our values follow the experimental trends at both qualitative and quantitative levels.

Comparison with previous theoretical studies on this process is possible only for the molecular complexes[35] and for the reaction path leading to the insertion intermediate in the case of titanium.[32] We would like to underline that the previous ab initio MP4(SDTQ)/6-31G**//MP2/6-31G** investigation[32] of Ti^+ reaction with ammonia includes the metal ion in its doublet state, while in the present study we refer to titanium in its quartet ground state. However, the discrepancy in the reported energy differences is too large to be ascribed to this difference in the reference state.

3.2. M^+ Insertion into C−H Bond. The experimental studies[7−9] of the reaction of M^+ (M = Ti, V, Cr) with methane suggest again that the mechanism of oxidative addition is operative to form the intermediate $HMCH_3^+$. From this intermediate the dehydrogenation reaction is predicted to be the most energetically favorable. Table 4 lists our results together with available theoretical[34,35] and experimental[7−9] energetic parameters.

Table 4. Relative Energies of M^+-CH_4 (ΔE), HM^+-CH_3 (ΔE_1), and $MNH_2^+ + H_2$ (ΔE_2) Products with Respect to the Ground State of Reactants[a]

system	method	ΔE	ΔE_1	ΔE_2
$Ti^+(^4F) + CH_4$	B3LYP/DZVP[b]	−22.21	−7.09	21.96
	CASPT2[c]		1.1	
	MP4//MP2[d]	−73.1	−20.7	
	expt[e]		−11.5	16.8 ± 1.8
$V^+(^5D) + CH_4$	B3LYP/DZVP[b]	−15.09	14.43	37.70
	CASPT2[c]		18.0	
	expt[f]		11.76	34.1 ± 1.6
$Cr^+(^6D) + CH_4$	B3LYP/DZVP[b]	−13.10	38.75	53.68
	CASPT2[c]		51.5	
	expt[g]		42.0	56.50 ± 3.7

[a] Ground states of products are Ti^+-CH_4 (^4A), $H-Ti^+-CH_3$ (^2A), $TiCH_2^+$ (^3A) + H_2, V^+-CH_4 (^5A), $H-V^+-CH_3$ (^3A), VCH_2^+ (^3A), Cr^+-NH_3 (^6A), $H-Cr^+-NH_2$ (^4A), and $CrCH_2^+$ (^4A) + H_2. [b] The basis sets refer to the metal atom. [c] Reference 33. [d] Reference 32. These values of ΔE are calculated with respect to the doublet excited state of reactants. [e] Reference 8. [f] Reference 7. [g] Reference 9.

The structures of stationary points, in the high- and low-spin states, are shown in Figures 5, 6, and 7, while the corresponding PESs are shown in Figure 8.

The envisioned mechanism includes formation, in the entrance channel, of the long-lived ion−induced-dipole complex (**I**), which subsequently yields the insertion intermediate (**II**) by migration of a hydrogen atom corresponding to the transition state TS1. The methane complexes (**I**) have the tridentate structure shown in Figures 5a−7b, with C_{3v} symmetry, in both the low- and high-spin states, except for the vanadium complex in its high state, which possesses a C_{2v} bidentate structure. All other possible bidentate and tridentate structures for the same complexes are transition states as confirmed by the vibrational analysis. The hypothesis of the existence of the intermediate (**II**) was reinforced by the detection, in the case of methane activation by V^+, of a species with thermochemical properties consistent with the structure of (**II**).[7] Along the path another ion−induced-dipole complex (**III**) is found in the exit channel for H_2 elimination. This species is obtained from (**II**) through the tight four-center transition state TS2. All the mentioned species were localized along the potential energy surfaces of the low- and high-spin states, except the high-spin transition states, TS1s, for which the search was unsuccessful despite the numerous strategies pursued to find them. To verify if this failure was due to the method used, we tried to find these TSs employing the MP2 tool, again without success. On the contrary, along the low-spin surfaces, M^+ ions insert into the C−H bond with a relatively small barrier, relative to the MCH_4^+ complexes, and lead to the insertion intermediates, which are higher in energy with respect to the same complexes. Thus, the reactivity along the doublet, the triplet, and the quartet paths, for titanium, vanadium, and chromium, respectively, is expected to be much larger than that along the corresponding high-spin surfaces. Then, after formation of the $H-M^+-CH_3$ complex, the reaction moves toward product formation conserving spin.

Such a situation also occurs for the interaction of scandium cation with methane, but due to a small energy difference between Sc^+ ^3D and ^1D states the possibility that the reaction evolves to product formation conserving spin can be hypothesized. Thermochemical arguments also support the occurrence

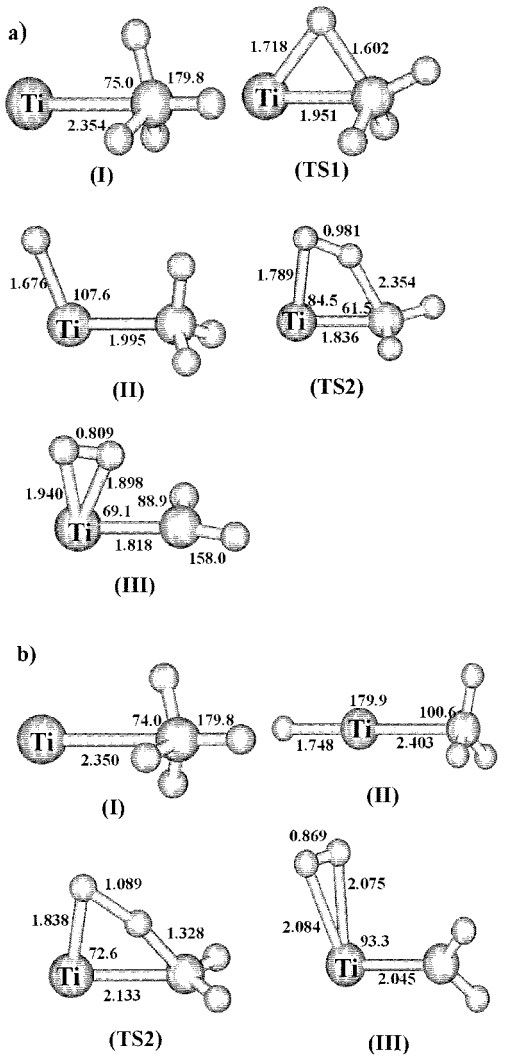

Figure 5. Geometric parameters of minima and transition states on the B3LYP/DZVP doublet (a) and quartet (b) potential energy surfaces for the reaction of Ti^+ with CH_4. Bond lengths are in angstroms and angles in degrees.

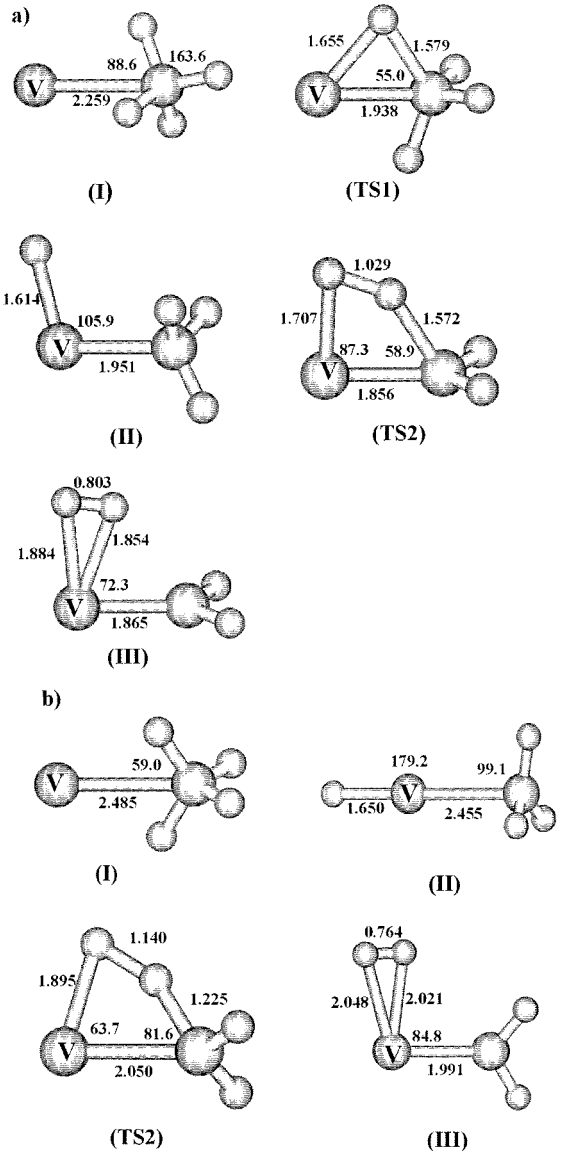

Figure 6. Geometric parameters of minima and transition states on the B3LYP/DZVP triplet (a) and quintet (b) potential energy surfaces for the reaction of V^+ with CH_4. Bond lengths are in angstroms and angles in degrees.

of spin-allowed processes. Indeed, for vanadium and chromium the crossing would occur at an energy above that of the ground-state reactants and, for all the considered cations, along the low-spin surface there is no barrier in excess of the endothermicity.

At higher energies the production of MH^+ and MCH_3^+ species is proposed to occur through metal−carbon or metal−hydrogen bonds cleavage of the intermediate (**II**) in its ground state. The energetics of these processes is reported in Table 5. Our prediction accounts well for the experimental results, especially for titanium and vanadium, while the difference between our results and experiment for methane activation by the chromium cation is somewhat greater.

4. Comparison between PESs

In this section we summarize the findings of both our[31] and previous theoretical calculations[27−29] concerning the behavior of the PESs for the dehydrogenation reaction of water, ammonia, and methane by Sc^+, Ti^+, V^+, and Cr^+ metal cations. As can be seen in Figures 5 and 8 and on the basis of previous results,[27−29,31] the reaction paths, as well as geometric structures of key points, are similar in all the considered cases, especially along the low-spin-state PESs.

Despite the qualitative similarity between the reaction paths, there are significant differencies in the energetics. The thermodynamic stability trends, with respect to ground-state asymptotes for the ion−dipole complexes (**I**), the transition states leading to insertion intermediates, TS1, the insertion intermediates (**II**), and the ground-state products are drawn in Figures 9−11. For each stationary point considered only the relative energy of the most stable high- or low-spin species has been reported. First of all, the interaction between M^+ and the ligand in the ion−molecule complex (**I**) is strongest in the case of ammonia and decreases on going to water and methane. As previously described in detail,[63,64] the magnitude of the bonding between the metal ions and the simple noninserted ligand is not only

(63) Rosi, M.; Bauschlicher, C. W., Jr. *J. Chem. Phys.* **1989**, *90*, 7264.
(64) Langhoff, S. R.; Bauschlicher, C. W., Jr.; Partridge, H.; Sadupe, M.; Rosi, M. *J. Phys. Chem.* **1991**, *95*, 10677.

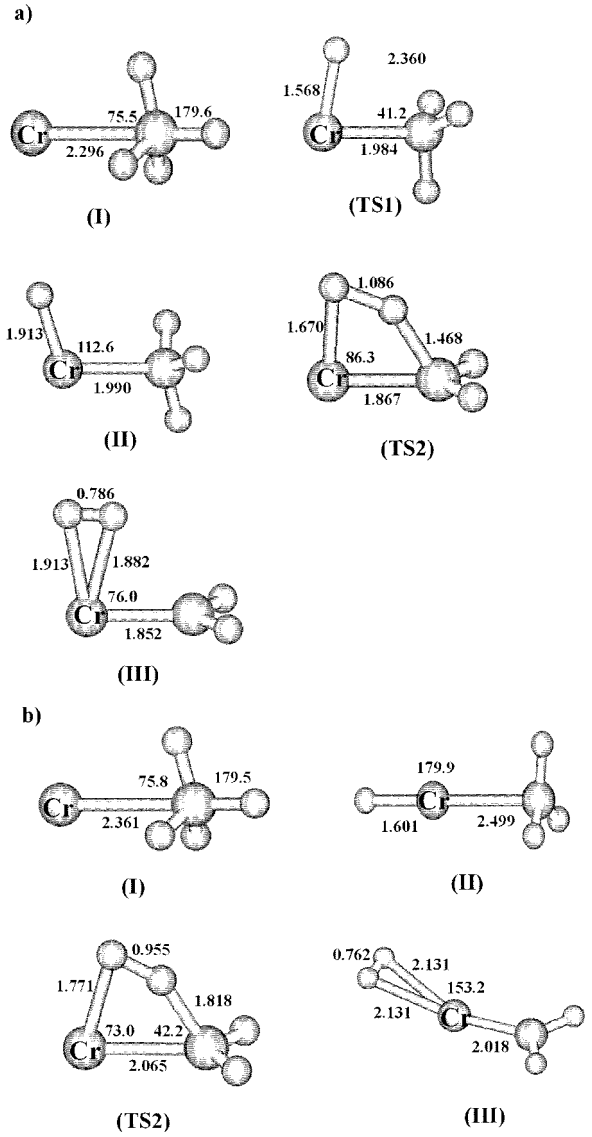

Figure 7. Geometric parameters of minima and transition states on the B3LYP/DZVP quartet (a) and sextet (b) potential energy surfaces for the reaction of Cr^+ with CH_4. Bond lengths are in angstroms and angles in degrees.

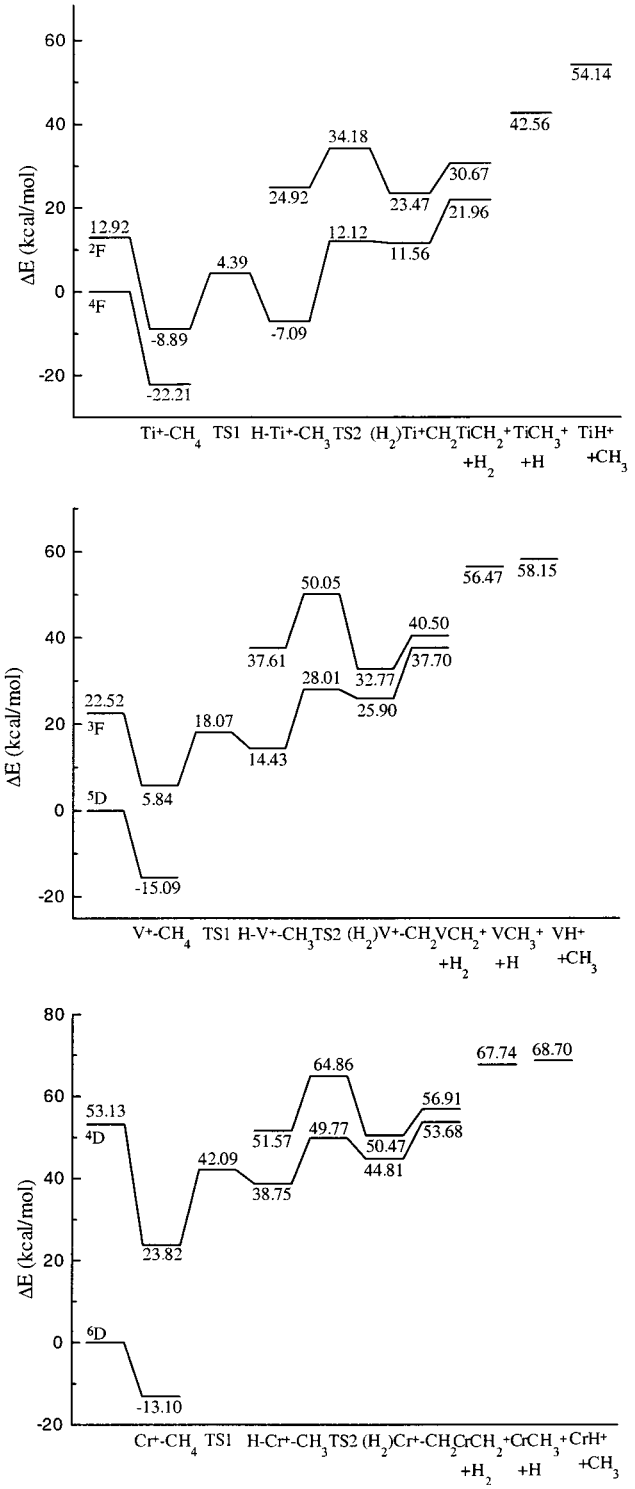

Figure 8. B3LYP/DZVP high- and low-spin potential energy surfaces for the reaction of Ti^+, V^+, and Cr^+ with NH_3. Energies are in kcal/mol and relative to the ground-state reactants.

electrostatic in nature; the magnitude of the binding energy is determined by a balance between the electrostatic interaction and Pauli repulsion. Indeed, increase of Z would lead to shorter metal−ligand bond distances and larger binding energies proceeding from left to right in the row. The increasing M−X bond distances from oxygen, to nitrogen, and to carbon (see Figures 1−3 and 5−7 and refs 27−29 and 31) and the decreasing values of the dipole moments for water, ammonia, and methane are inconsistent with the observed trends collected in Figures 9a−11a. The available mechanisms adopted by the metal cation to reduce Pauli repulsion, therefore, are responsible for the reported order of the values.

The next minimum along the surfaces is the low-spin H−M−XH_{n-1}complex, whose formation is the key step for all the considered processes. The formation of two M−L σ bonds is the outcome of the pairing of two metal electrons with two electrons originally occupying the X−H σ bonds and explains the enhanced stability of the low-spin hydrido complexes. As can be expected, the M−H bond distance decreases from left to right along the row, reflecting the decrease of the ionic radius. The M−X distance, on the other hand, decreases from Sc^+ to V^+ and then increases for Cr^+. The obvious conclusion, therefore, is that the evolution in ionic radius is not the only factor determining the stability of the considered species and covalent effects must be taken into account. The NBO analysis of these intermediates disagrees with the previous hypothesis of Hendrickx et al.[35] because it does not show any significant

Table 5. Relative Energies of $M-CH_3^+ + H$ (ΔE) and $MH^+ + CH_3$ (ΔE_1) Products with Respect to the Ground State of the Reactants[a]

system	method	ΔE	ΔE_1
$Ti^+(^4F) + NH_3$	B3LYP/DZVP[b]	42.56	54.14
	expt[c]	46.6 ± 2.8	50.5 ± 2.5
$V^+(^5D) + NH_3$	B3LYP/DZVP[b]	56.47	58.15
	expt[d]	54.7 ± 2.3	56.5 ± 0.9
$Cr^+(6D) + NH_3$	B3LYP/DZVP[b]	68.7	67.74
	expt[e]	74.7 ± 2.5	72.4 ± 2.1

[a] Ground states of the products are Ti^+-CH_3 (^3B) + H (^2S), TiH^+ ($^3\Delta$) + CH_3 (^2A), VCH_3^+ (^4B) + H (^2S), VH^+ ($^4\Delta$) + CH_3 (^2A), Cr^+-CH_3 (^5A) + H (^2S), and CrH^+ ($^5\Delta$) + CH_3 (^2A). [b] The basis sets refer to the metal atom. [c] Reference 8. [d] Reference 7. [e] Reference 9.

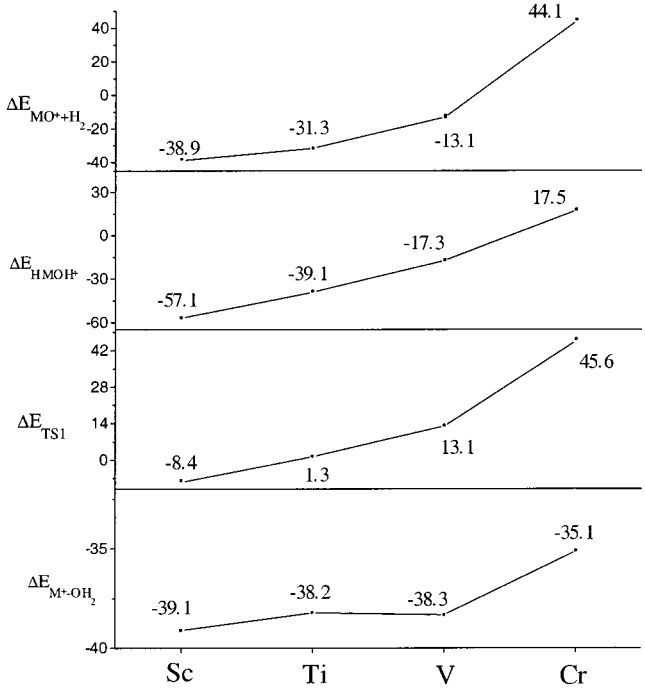

Figure 9. B3LYP/DZVP relative energies (kcal/mol) for the most stable (a) ion−dipole complexes, (b) transition states, (c) insertion intermediates, and (d) dehydrogenation products of the dehydrogenation reaction of water with respect to the ground-state asymptotes ($M^+ + H_2O$). Energies are in kcal/mol and relative to the ground-state reactants.

decrease of the occupation of the M−X bonding orbitals (all the occupations are in the range 1.999−1.980) and, consequently, there is not an increase of the occupation numbers of the antibonding orbitals along the row. Other factors can be invoked to explain the observed trends, as has been proposed[65−67] to interpret the bond energies of first-row transition metal hydride cations, MH^+. The first point to consider is the M^+ $4s^13d^{n-1}$ configuration and, then, the spin pair of the appropriate orbitals of the metals with those of the ligands to form the two σ bonds. When the ground state of the cation is $3d^n$, the effect of the promotion to an excited state is a weakening of the bond. Moreover, there is a change in the exchange terms of the energy because of the spin pairing of the electrons of the metal and, again, a weakening of the bond.

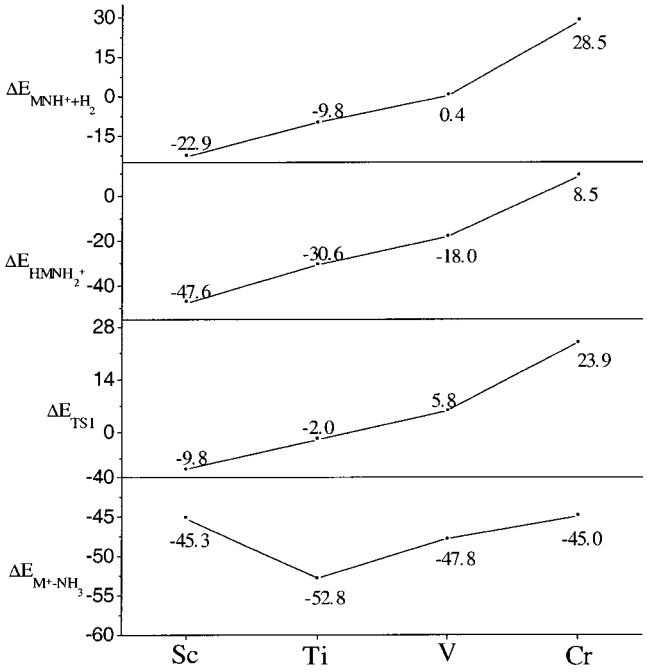

Figure 10. B3LYP/DZVP relative energies (kcal/mol) for the most stable (a) ion−dipole complexes, (b) transition states, (c) insertion intermediates, and (d) dehydrogenation products of the dehydrogenation reaction of water with respect to the ground-state asymptotes ($M^+ + NH_3$).

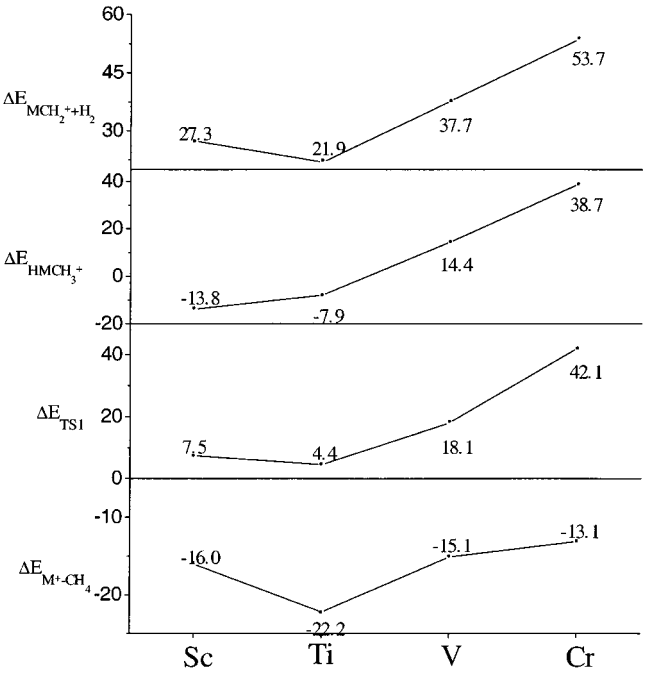

Figure 11. B3LYP/DZVP relative energies (kcal/mol) for the most stable (a) ion−dipole complexes, (b) transition states, (c) insertion intermediates, and (d) dehydrogenation products of the dehydrogenation reaction of water with respect to the ground-state asymptotes ($M^+ + CH_4$).

As previously postulated,[68] the presence of different numbers of lone pairs on the oxygen, nitrogen, and carbon atoms can be considered responsible for the decrease, from water, to ammonia, and to methane, of the stability of the hydrido intermediates observed along the paths for the three ligands (see Figures 9c−11c). Indeed, the possibility of oxygen to form two dative bonds,

(65) Schilling, J. B.; Goddard, W. A., III; Beauchamp, J. L. *J. Am. Chem. Soc.* **1986**, *108*, 582.
(66) Armentrout, P. B.; Halle, L. F.; Beauchamp, J. L. *J. Am. Chem. Soc.* **1981**, *103*, 6501.
(67) Elkind, J. L.; Armentrout, P. B. *Inorg. Chem.* **1986**, *25*, 1080.
(68) Armentrout, P. B.; Kickel, B. L. In *Organometallic Ion Chemistry*; Freiser, B. S., Ed.; Kluwer: Dordrecht, 1996; pp 1−45.

Table 6. Equilibrium Geometry Parameters for MXH_{n-2} Low-Spin Dehydrogenation Products at the B3LYP/DZVP Level of Theory[a]

product	metal	M–X	X–H	M–X–H
MO^+	Sc	1.636[b]		
	Ti	1.580[c]		
	V	1.545[c]		
	Cr	1.586[c]		
MNH^+	Sc	1.712	1.020	
	Ti	1.672	1.034	
	V	1.649	1.038	
	Cr	1.716	1.033	
MCH_2^+	Sc	1.887	1.099	123.1
	Ti	1.860	1.095	123.4
	V	1.872	1.094	123.2
	Cr	1.859	1.093	121.5

[a] Bond lengths are in angstroms and angles in degrees. [b] References 26−28 and 30. [c] References 26−28.

one in the case of nitrogen and none for methane, corresponds to a gradual weakening of the bond strength. The analysis of the bond shows the existence of a triple bond between M and O, a double bond between M and N, and a single bond between M and C. The exception to this rule is represented by chromium, for which there is evidence of only a partial sharing of the second lone pair of oxygen and of the lone pair of nitrogen with a consequent decrease in bond strength.

The difference in energy between the reactants and the transition state of the rate-determining step is defined as the activation energy for the reaction. The curves for these quantities are reported in Figures 9b−11b. Since the H−X bond is practically broken and the M−H bond formed, the position of the barrier heights follows the same trend as the stabilization energies of the insertion intermediates.

Finally, we briefly comment on the trends of the stability of dehydrogenation products as shown in Figures 9d−11d. Bond lengths and angles of the most stable low-spin dehydrogenation products are reported in Table 6. Also in this case a gradual decrease of the bond length in going from scandium to vanadium ions is observed, reflecting the decrease in the extent of the metal orbital involvement and then an increase for chromium ion. By contrast, the stabilities decrease from left to right in the row. This effect can be ascribed to the loss of d−d exchange energy upon bonding as the number of metal d electrons increases. The nature of the metal−oxygen, −nitrogen, or −carbon bond can be rationalized considering the formation of two covalent bonds by the metal with the unpaired electrons of oxygen and nitrogen enhanced by the donation of electron density from the lone pair of 2p electrons into empty d orbitals. The net result is the existence of a triple bond in these species for the first three transition metals. The situation changes when the metal valence orbitals are not empty as in the case of chromium ion. An analysis of the bond reveals that the donation of electron density from the lone pairs is only partial in this case. In considering the bonding between the transition metal and the carbon atom of the CH_2 group, we find similarities in behavior, due to the presence of two 2p unpaired electrons with formation of two covalent bonds. Unlike oxygen and nitrogen, carbon has no lone pair to share with the metal, thus accounting for the weaker M−C bond strength.

5. Conclusions

The reaction of Ti^+, V^+, and Cr^+ with ammonia and methane have been investigated in detail at the B3LYP/DZVP level of theory, considering both the low- and high-spin potential energy surfaces, and compared with previous analogous studies of the reactions of the same cations with water and of the Sc^+ ion with the same molecules.

The proposed experimental qualitative behavior of the potential energy surfaces for the insertion reaction of early and middle first-row transition metal ions into the O−H, N−H, and C−H bonds of water, ammonia, and methane, respectively, is confirmed, and quantitative details are given. In the first step the reactants yield a stable ion−molecule complex from which the insertion intermediate is formed through a transition state that corresponds to the migration of a hydrogen atom toward the metal ion. From the insertion intermediate a molecular hydrogen complex is obtained via a tight four-center transition state. Then, without an energy barrier, the complex decomposes to give the reaction products directly.

The key reaction intermediates, $H-M^+-XH_{n-1}$, surmised by experimentalists have been localized and characterized. Because of the excited nature of this intermediate with respect to the ground state of the reactants, the reactions are presumed to occur via a crossing from the high-spin to the low-spin surface. The need for an intersystem crossing can justify the low efficiency of these reactions.

By using arguments based on energetics, in the case of methane, it is suggested that the reaction takes place more easily along the low-spin potential surface, without an inefficient intersystem crossing. On the other hand, the experimental data evidence that the low-spin states are much more reactive, by about 2 orders of magnitude, than the high-spin ground states.

The information gained from the comparison between the behavior of the PESs for different metal ions and ligands may provide a useful insight into the interaction of transition metals with small molecules and improve the coordination chemist's view of metal−ligand bonding. Work is in progress to perform analogous studies for the other transition metal cations of the first row.

Acknowledgment. Financial support from the Università degli Studi della Calabria and MIUR is gratefully acknowledged.

JA0112487